Linking Surface Precipitation in Fe-Au Alloys to Its Self-healing Potential During Creep Loading

Sun, W. W.; Fang, H.; van Dijk, N. H.; van der Zwaag, S.; Hutchinson, C. R.

DOI
10.1007/s11661-017-4025-x

Publication date
2017

Document Version
Final published version

Published in
Metallurgical and Materials Transactions A - Physical Metallurgy and Materials Science

Communication

Linking Surface Precipitation in Fe-Au Alloys to Its Self-healing Potential During Creep Loading

W.W. SUN, H. FANG, N.H. VAN DIJK, S. VAN DER ZWAAG, and C.R. HUTCHINSON

The precipitation of Au-rich precipitates on the external surfaces of Fe-Au alloys has been studied by scanning and transmission electron microscopy. The surface precipitates formed at elevated temperatures are found to self-organize in regular patterns and their growth rate is determined quantitatively. The observed surface precipitation at a free surface is compared to the precipitation at the internal surface of grain boundary cavities induced by creep loading. A close agreement between both processes is observed.

DOI: 10.1007/s11661-017-4025-x

While the field of (ferrous) metallurgy has a history of many centuries, the very nature of the materials and their many transformation modes leads to a continuous stream of discoveries even until today. In recent years, two new (intentional) discoveries were made due to dedicated research: (i) transient solid-state precipitation of new phases on the surface of binary and ternary alloys[1] and (ii) the self-healing of creep damage in steels and related alloys[2–4] due to the autonomous filling of creep loading induced cavities leading to a significant life extension. Until now, the two phenomena were studied in isolation. The current work aims to bridge the two phenomena by linking the surface precipitation of a Fe-Au alloy to its capability to heal creep damage.

W.W. SUN and C.R. HUTCHINSON are with the Department of Materials Science and Engineering, Monash University, Clayton 3800, VIC, Australia. Contact e-mail: christopher.hutchinson@monash.edu H. FANG is with the Fundamental Aspects of Materials and Energy group, Faculty of Applied Sciences, Delft University of Technology, Mekelweg 15, 2629 JB Delft, The Netherlands and also with the Novel Aerospace Materials group, Faculty of Aerospace Engineering, Delft University of Technology, Kluyverweg 1, 2629 HS, Delft, The Netherlands. N.H. VAN DIJK is with the Fundamental Aspects of Materials and Energy group, Faculty of Applied Sciences, Delft University of Technology. S. VAN DER ZWAAG is with the Novel Aerospace Materials group, Faculty of Aerospace Engineering, Delft University of Technology.
Manuscript submitted December 7, 2016.

Traditional bulk (internal) precipitation reactions that lead to a significant increase in strength are well known in both non-ferrous and ferrous alloys and are used to design new alloys with improved mechanical properties. However, only recently it has been discovered that there are alloys where the annealing conditions may be tuned to generate precipitates with a high areal surface density (10^{10}-10^{11} m^{-2}) on the external surface of the sample (surface precipitation) at elevated temperatures.[1] The observed surface precipitation shows a surprising periodicity that is not directly related to the microstructure. Surface precipitation (which may be enhanced by concurrent surface segregation) occurs in competition with traditional bulk precipitation and the subsurface volume acts as a huge reservoir of solute atoms for the surface precipitation reaction. For a system to be capable of surface precipitation, there must be a lower energy barrier for precipitation on the surface than for internal (bulk) precipitation. Precipitates exhibiting a significant lattice misfit with the bulk matrix may be good candidates. These studies on precipitate formation on free surfaces by segregation from the bulk show some similarities (but also significant differences) with island formation and self-organization of atoms individually deposited on free surfaces during processes such as physical vapor deposition.[5–8]

On the other hand, research into the development of alloys with a superior creep resistance has used the preferred surface precipitation of secondary phases on the free surface of internal creep cavities as a strategy to achieve an autonomous repair of creep damage, resulting in significant extension of the creep lifetime. Conventional creep-resistant steels have a surprisingly long lifetime given the ultra-demanding combination of requirements in load, temperature, and lifetime.[9–13] However, even the best creep-resistant steels fail at some stage. The failure mode depends on the actual loading conditions, but generally starts with the formation of isolated creep cavities (with dimensions of 1-3 μm) at the load-bearing grain boundaries. These isolated creep cavities then grow into merged cavities that develop into micro-cracks and finally result in macro-cracks that lead to failure. To stop the accumulation of early creep damage to catastrophic dimensions, it is clear that this requires a filling of the creep cavities at the grain boundary before they reach critical dimensions sufficient for pore merging and micro- and macro-crack formation. Hence, the conceptual approach to create self-healing creep steels has been to search for systems in which the formed creep cavities could be filled by precipitation. To exploit solid-state precipitation for this purpose, the system must have a solute element with a maximum solubility at temperatures well above the creep temperature that shows a strongly reduced solubility at the creep temperature. It has been shown[2,3,14] that a preference for surface precipitation rather than bulk precipitation requires that the precipitation is associated

Published online: 27 February 2017

with a large increase in molar volume (providing a strong preference for surface precipitation in the creep cavities rather than traditional bulk precipitation). Preferentially, the solute atoms involved in the precipitate formation should not have a tendency to form compounds with any of the interstitial (carbon, nitrogen, or sulfur) or substitutional alloying elements, as this leads to premature immobilization of the surface precipitating element.

These requirements for creep cavity filling by solid-state precipitation[4] are identical to those for surface precipitation.[1] The clearest demonstration of self-healing in creep steels (or model alloys thereof) has been obtained for binary Fe-3Au (wt pct), which meets all the requirements.[2,3] Although the formation of Au-rich precipitates on the surface of a high purity Fe-Au alloy has been demonstrated by XPS,[14] no information is available on their topology.

The current study aims to demonstrate the link between these two previously unrelated developments—(external) surface precipitation on alloys[1] and creep cavity filling by (internal) surface precipitation during creep loading.[2–4] This link is demonstrated by considering the free outer surface precipitation of Au on undeformed samples of a high purity Fe-3Au (wt pct) model alloy and links the observations to the creep damage healing behavior of the same material.[2,15] To this aim, the unique X-ray nano-tomographic data[15] on unfilled, partially filled, and fully filled grain boundary cavities in creep-loaded Fe-3Au (wt pct) samples were re-analyzed to derive the precipitation density on the internal creep cavities, and these are compared with the densities directly measured on samples annealed at the same temperatures yet under stress-free conditions to induce external surface precipitation.

The same Fe-Au alloy as used in the creep damage healing research[2,3,15] is used for this surface precipitation study. The high purity Fe-Au alloy contains 2.87 wt pct Au (~1 at. pct Au) and a minimal amount of other interstitial and substitutional elements. The material was supplied by Goodfellow as cold-rolled sheet. For the surface precipitation studies, the samples were mechanically polished to an OPS finish (0.05 μm), encapsulated in quartz tubes after creating a vacuum of about 10^{-5} bar, heated in a two-zone tube furnace to 1143 K (870 °C) for 1 hour, followed by cooling to a lower temperature to induce surface precipitation during an isothermal heat treatment. Samples were annealed at 973 K, 873 K, 823 K, 773 K, and 673 K (700 °C, 600 °C, 550 °C, 500 °C, and 400 °C) for 30 minutes and subsequently characterized by scanning electron microscopy (SEM). In all cases, surface precipitation of Au was observed. A time series of surface precipitation was performed at 823 K (550 °C) to estimate the kinetics of the surface precipitate nucleation and growth. Selected samples were observed in transmission electron microscopy (TEM) using a Tecnei F20 field emission gun (FEG) TEM operating at 200 kV for measurements of the composition of the Au surface precipitates using energy-dispersive spectroscopy (EDS). These samples were prepared using a focussed ion beam (FIB) by first depositing a layer of Pt on the surface of the sample to protect the Au surface precipitates during milling. The TEM foils were milled using a FIB to prepare cross-sections through the Au surface precipitates. The conditions used for the creep damage healing studies are described in detail elsewhere and involve both macroscopic/microscopic studies of damage evolution[2,3] and the X-ray nanotomography studies of the actual creep damage pore-filling process with a resolution down to 25 nm.[15]

In Figure 1, Secondary Electron Images (SEI) of the external surfaces of the Fe-Au alloy are shown revealing quasi-periodic surface precipitation of Au particles. The samples in Figures 1(a) and (b) were held for 30 minutes at 1043 K (700 °C), and those of Figures 1(c) and (d) were held at 873 K and 773 K (600 °C and 500 °C), respectively. In all cases, extensive precipitation is observed at the external surface.

The precipitates are organized in regular structures and seem to be aligned along specific surface features. As shown in Figure 1(d), the precipitates appear to be aligned along steps formed by faceting of the surface during the heat treatment. This surface faceting will reflect the underlying crystallographic directions of the matrix grain, but these have not been studied in detail at this stage. However, this surface faceting does not appear to be the only feature affecting the patterning of the surface precipitates. As shown in Figure 1(c), some precipitates are clearly nucleated on the surface steps that run vertically in this image, but an array of aligned particles also runs horizontally in this image. Again, the alignment is expected to originate from the crystal orientation of the surface plane as the strain will be minimized for certain orientation relations between the Au-rich precipitates (*fcc*) and the matrix surface (*bcc*). The periodicity, observable in Figure 1(b), depends on the nucleation rate and will thereby be sensitive to the nominal Au concentration in the matrix and the temperature (*via* the diffusion rate). The phenomena causing the alignment and periodicity of the Au-rich surface precipitates and those in other metallic systems showing surface precipitation deserve further investigation.

There are a number of differences between the characteristics of Au surface precipitation in Fe-Au compared to other metal alloys such as Al-Si and Al-Si-Ge.[1] Figure 1(a) illustrates that the sizes and number densities of Au surfaces precipitates in the Fe-Au system varies from grain to grain and precipitate-free zones may form around the grain boundaries. Figures 1(b) through (d) demonstrate that the nucleation of Au precipitates is sensitive to the topology of the surface and may result in alignment of particles. In the case of the Al-Si-based systems,[1] the distribution of Si surface precipitates is extremely uniform, including the near-grain boundary regions, and relatively independent of grain orientation. Not surprisingly, the details of the surface nucleation and surface growth of precipitates are system dependent.

To obtain an estimate of the surface precipitation kinetics at 823 K (550 °C) (the same temperature as the creep loading studies to be subsequently discussed), a time series of 5, 10, and 20 minutes was performed,

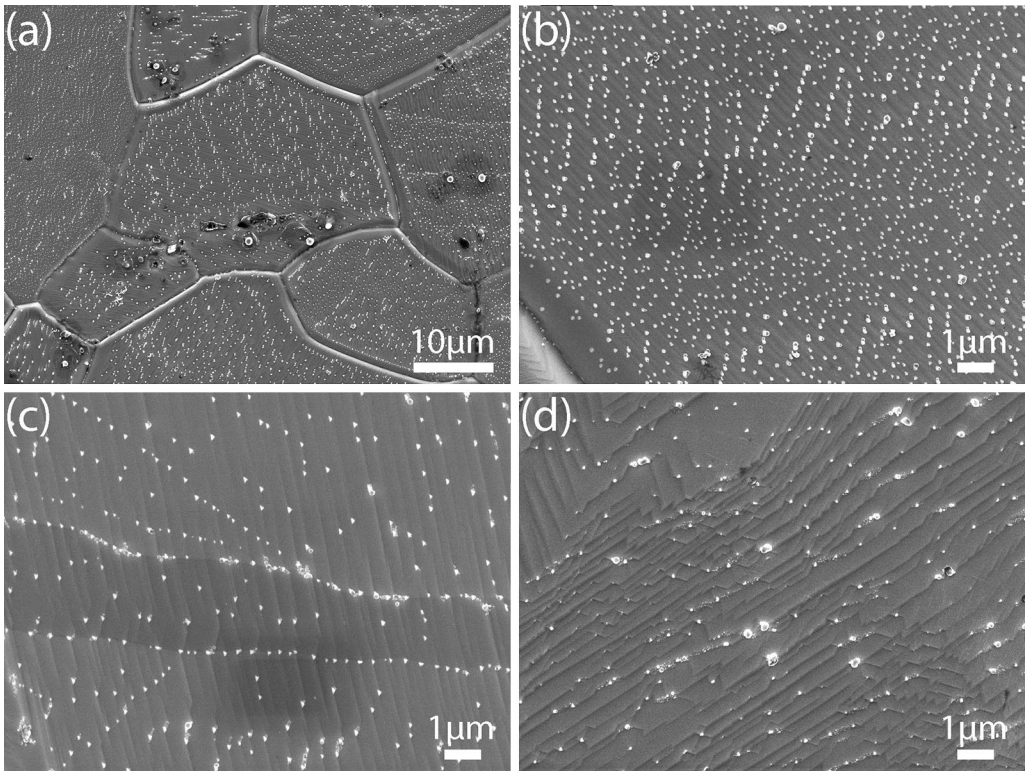

Fig. 1—SEI-BSE images of the Fe-Au alloy treated for 60 min at 1143 K (870 °C), followed by 30 min annealing at (*a* and *b*) 973 K (700 °C), (*c*) 873 K (600 °C), and (*d*) 773 K (500 °C), respectively. The white features are the Au particles on the external surfaces of the alloy.

followed by a rapid quenching into water (and fracture of the quartz tube). After this treatment, the surfaces were quantitatively characterized using SEM. The time evolution of the surface precipitate number density, areal width, and areal length is shown in Figures 2(a) through (c). Each data point corresponds to a single grain and combines the results of 20-30 particles within that grain measured from SEM images like those (but higher magnification) shown in Figure 1. 5-10 grains were characterized per aging time. The surface precipitates shown in Figures 1(b) through (d) appear relatively equiaxed, but this does not apply to all grains. Other grains exhibit surface precipitates with aspect ratios up to approximately 2-3 and this is the reason for reporting a length and width in Figure 2. The surface precipitation process in the Fe-Au system is extremely fast, consistent with the earlier XPS experiments[3] and the observations made in the Al-Si system.[1]

From Figure 2, it is possible to make an estimate of the minimum nucleation and growth rates of the Au precipitates on the external surface of the alloy during aging at a temperature of 823 K (550 °C). The areal nucleation rate must be faster than 3×10^9 m^{-2} s^{-1}. The minimum areal growth rate may be estimated by considering an average particle area of $A = 1 \times 10^4$ nm^2 after 5 minutes (Figure 2(d)) (corresponding to a particle radius of $R \approx 50$-60 nm). When we consider a 2D diffusion-controlled elliptical growth process with a diffusivity, D, the particle size is expected to scale with time as $R_1 \propto R_2 \propto (Dt)^{1/2}$ for both precipitate axes, resulting in a linear time dependence for the area $A = \pi R_1 R_2 \propto Dt$ and a constant growth velocity for the precipitate area $\mathrm{d}A/\mathrm{d}t$. The experimental value of $A \approx 1 \times 10^4$ nm^2 after 5 minutes then corresponds to a constant areal growth rate of $\mathrm{d}A/\mathrm{d}t \approx 30$ nm^2/s. Considering that the growth anisotropy is only moderate (maximum aspect ratio of 2-3), we can estimate an average radial growth rate of $\mathrm{d}\langle R\rangle/\mathrm{d}t = (\mathrm{d}A/\mathrm{d}t)/(4\pi A)^{1/2} \approx 0.1$ nm/s. This radial growth rate is however time-dependent and therefore only an estimate for the average linear growth rate at a time of 5 minutes. In comparison, for the Al-Si system at similar temperatures, the average interface migration rate was estimated to be 10 nm/s.[1] However, the areal number density of precipitates in the Al-Si system was two orders of magnitude lower than found for the Fe-Au system (Figure 2(a)), and hence the competition between surface nucleation and surface growth is found to be quite different for the two systems. A common feature of the surface precipitation in different alloys is that it progresses extremely quickly due to the fast surface diffusion.

However, for self-healing by a filling of creep cavities by precipitation, the volumetric growth rate is more important than the areal growth rate. To estimate this quantity from the kinetics of surface precipitation on external surfaces, it is necessary to also know the height of the Au precipitates that are formed on the free surface (shown in Figure 2). From the surface of the Fe-Au sample treated for 10 minutes at 823 K (550 °C), a transmission electron microscopy (TEM) foil has been produced using a focused ion beam (FIB). The surface

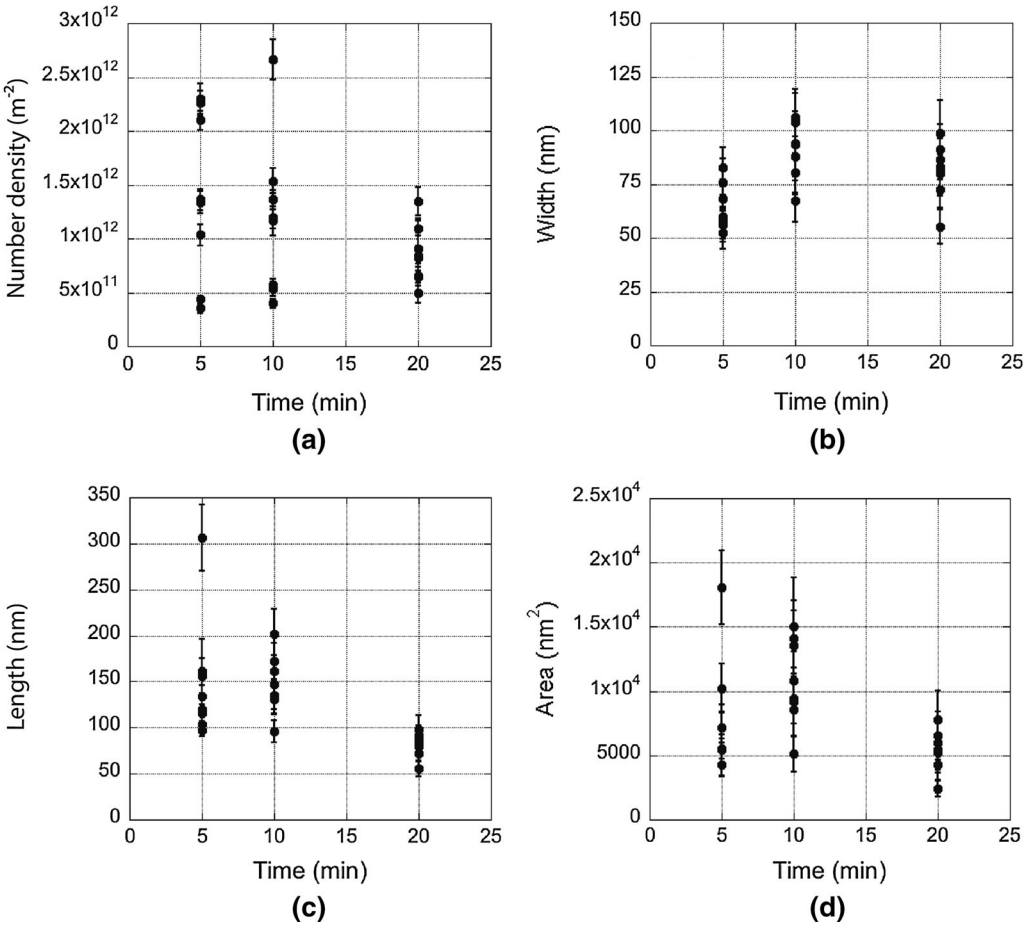

Fig. 2—Values of the (*a*) number density, (*b*) length, (*c*) width, and (*d*) area of the surface precipitates in the Fe-Au alloy solution treated for 60 min at 1143 K (870 °C), followed by holding for various times at 823 K (550 °C).

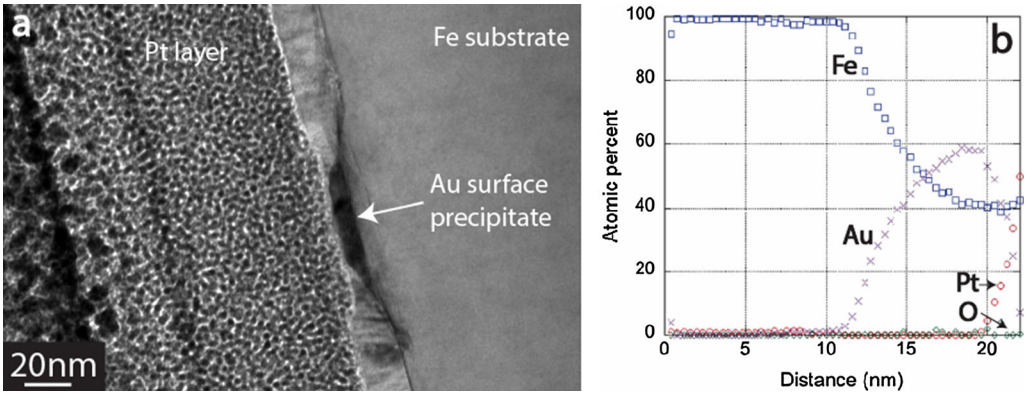

Fig. 3—(*a*) BF-TEM image of the Au precipitate in a foil prepared using a FIB from the Fe-Au sample treated for 10 min at 773 K (500 °C) and then water quenched, (*b*) EDS line profile across the substrate, particle, and Pt coating layer.

was coated with Pt prior to the FIB milling to protect the Au surface precipitate and surrounding area from Ga ion damage. Figure 3(a) shows a bright field (BF) TEM image of the sample revealing the presence of a surface precipitate. This particular surface precipitate is approximately 40-60 nm long and about 10 nm thick. Consistent with the observations made for the surface precipitation of Si in the Al-Si system,[1] the Au precipitates rise above the surface by a maximum height of about 10 pct of the largest lateral dimension. Assuming a circular disk geometry for this precipitate, an estimated volume $V \approx 2 \times 10^4$ nm^3 is obtained. An EDS line profile obtained in TEM across the precipitate in Figure 3(a) is shown in Figure 3(b). It is observed that

Table I. Volume Number Density $n_V = (1/V)\sum_i N_{p,i}$ of Gold Precipitates Subdivided in Different Shapes and Areal Number Density $n_A = (1/A_{cav})\sum_i N_{p,i}$ for Creep-Failed Samples Loaded at Different Stress Levels (and Hence Different Failure Times) at a Temperature of 823 K (550 °C)

		n_V						n_A	Δ_A
Stress (MPa)	Failure Time (h)	Sphere (m^{-3})	Equiaxed (m^{-3})	Rod (m^{-3})	Sheet (m^{-3})	Complex (m^{-3})	Total (m^{-3})	Total (m^{-2})	Total (m)
60	642	4.7×10^{13}	1.9×10^{13}	4.2×10^{13}	6.2×10^{13}	4.2×10^{12}	1.7×10^{14}	5×10^{10}	4.5×10^{-6}
80	376	5.9×10^{14}	1.2×10^{14}	4.3×10^{14}	1.6×10^{14}	1.6×10^{13}	1.3×10^{15}	4.5×10^{11}	1.5×10^{-6}
100	210	4.9×10^{14}	8.9×10^{13}	2.3×10^{14}	1.4×10^{14}	1.3×10^{13}	9.3×10^{14}	4.6×10^{11}	1.5×10^{-6}
117	57	5.4×10^{14}	8.3×10^{13}	3.0×10^{14}	2.0×10^{14}	1.4×10^{13}	1.1×10^{15}	1.14×10^{12}	0.9×10^{-6}

In the determination of the areal cavity surface, the complex shaped cavities formed at the final creep stage were excluded. The average spacing between the well-developed precipitates on the creep cavity surface amounts to $\Delta_A = 1/\sqrt{n_A}$.

the Au composition reaches a maximum of approximately 60 at. pct Au with the balance Fe. At a temperature of 823 K (550 °C), the equilibrium composition of Au precipitates in the Fe-Au system is approximately 80 at. pct,[3] demonstrating that some solute trapping of Fe takes place during the rapid surface precipitation process. The higher than equilibrium Fe concentration observed in the precipitates indicates that they have grown under conditions of mixed interface and diffusion control.

These surface precipitation data from experiments on external surfaces are now compared with the results obtained from the X-ray nanotomography experiments on the creep-loaded samples showing surface precipitation on the internal creep cavity surfaces.[15] Table I shows the volume number density determined by tomography measurements of the same Fe-Au alloy after creep failure for different levels of loading stress at a temperature of 823 K (550 °C). In order to compare the number density with our present measurement, the volume number density $n_V = \frac{1}{V}\sum_i N_{p,i}$ was translated to an areal number density

$$n_A = \frac{1}{A_{\text{cav}}}\sum_i N_{p,i} = \frac{V}{A_{\text{cav}}} n_V = \frac{1}{S_{v,\text{cav}}} n_V, \qquad [1]$$

where $S_{v,\text{cav}} = A_{\text{cav}}/V$ is the specific surface of the cavity area A_{cav} per unit of sample volume V. The effective number densities are also shown in Table I. It can be seen that the areal number density (n_a) determined by tomography measurement is slightly smaller, but within one order of magnitude of that derived from present surface precipitation experiments (Figure 2(a)). The difference is attributed to the difference in experiment time between the creep experiments probing the internal surfaces (hundreds of hours) and the surface precipitation at the external surfaces in present work (ten minutes). The number density in the creep-loaded samples is expected to be lower as a result of coarsening and coalescence.

According to the X-ray tomography measurement on gold precipitation inside creep cavities, the time evolution of the volume V of spherical and equiaxed gold precipitates corresponds to $V = Ct^{0.8}$, where $C = 5.1 \times 10^3$ nm^3 s$^{-0.8}$. For a specific time of 5 minutes, the precipitate volume is $V \approx 5 \times 10^5$ nm^3. Assuming a disk-shaped precipitate with a characteristic value of $h/D \approx 1/10$ at a time of 5 minutes, then the precipitate volume $V = Ah = \pi D^2 h/4 \approx \pi D^3/40 \approx 5 \times 10^5$ nm^3 provides an estimate for the area $A = \pi D^2/4 \approx (\pi/4)^{1/3}(10V)^{2/3} \approx 3 \times 10^4$ nm^2. Again, assuming a constant areal growth rate, this corresponds to $dA/dt \approx 100$ nm^2/s. This estimate is of comparable magnitude to the value obtained for the surface precipitation at the external surface ($dA/dt \approx 30$ nm^2/s), demonstrating that the underlying physical principles for surface precipitation on external and internal surfaces are the same.

The solid-state precipitation of Au-rich precipitates on the external surfaces of an Fe-Au alloy is demonstrated. This alloy composition has previously been shown to exhibit self-healing ability during creep loading as a result of the filling of creep cavities by solid-state precipitation on the internal surfaces of creep cavities. The growth rates of the precipitates forming on the external surfaces and on the internal surfaces of the creep cavities are shown to be similar pointing at a mechanistic link between the previously separate studies of surface precipitation and self-healing during creep of metallic alloys. Hence, the relatively easy study of external surface precipitation may be useful for screening systems potentially capable of self-healing by creep cavity filling during loading and for estimating the nucleation and growth rates of such precipitates which must be compatible with the timescale of creep cavity formation for self-healing to be effective.

We thank Shasha Zhang for assistance with the sample preparation and fruitful discussions. Haixing Fang is financially supported by a grant from the China Scholarship Council (CSC). WWS and CRH gratefully acknowledge the use of the facilities in the Monash Centre for Electron Microscopy (MCEM) for the SEM and TEM reported in this contribution.

REFERENCES

1. Y. Chen, X.Y. Fang, Y. Brechet, and C.R. Hutchinson: *Acta Mater.*, 2014, vol. 81, pp. 291–303.
2. S. Zhang, C. Kwakernaak, W.G. Sloof, E. Brück, S. van der Zwaag, and N.H. van Dijk: *Adv. Eng. Mater.*, 2015, vol. 17, pp. 598–603.

3. S. Zhang, K. Kwakernaak, F.D. Tichelaar, W.G. Sloof, M. Kuzmina, M. Herbig, D. Raabe, E. Brück, S. van der Zwaag, and N.H. van Dijk: *Metall. Mater. Trans. A*, 2015, vol. 46A, pp. 5656–70.
4. S. Zhang, H. Fang, M.E. Gramsma, C. Kwakernaak, W.G. Sloof, F.D. Tichelaar, M. Kuzmina, M. Herbig, D. Raabe, E. Brück, S. van der Zwaag, and N.H. van Dijk: *Metall. Mater. Trans. A*, 2016, vol. 47A, pp. 4831–44.
5. W.G. Cullen and P.N. First: *Surf. Sci.*, 1999, vol. 420, pp. 53–64.
6. M.M.J. Bischoff, T. Yamada, A.J. Quinn, R.G.P. van der Kraan, and H. van Kempen: *Phys. Rev. Lett.*, 2001, vol. 87, p. 246102.
7. S. Rohart, Y. Girard, Y. Nahas, V. Repain, G. Rodary, A. Tejeda, and S. Rousset: *Surf. Sci.*, 2008, vol. 602, pp. 28–36.
8. C.S. Casari, S. Foglio, F. Siviero, A. Li Bassi, M. Passoni, and C.E. Bottani: *Phys. Rev. B*, 2009, vol. 79, p. 195402.
9. M.F. Ashby, C. Gandhi, and D.M.R. Taplin: *Acta Metall.*, 1979, vol. 27, pp. 699–729.
10. M. Yoo and H. Trinkaus: *Metall. Mater. Trans. A*, 1983, vol. 14A, pp. 547–61.
11. I.W. Chen and A.S. Argon: *Acta Metall.*, 1981, vol. 29, pp. 1321–33.
12. P. Shewmon and P. Anderson: *Acta Mater.*, 1998, vol. 46, pp. 4861–72.
13. M.E. Kassner and T.A. Hayes: *Int. J. Plast.*, 2003, vol. 19, pp. 1715–48.
14. S. Zhang, G. Langelaan, J.C. Brouwer, W.G. Sloof, E. Brück, S. van der Zwaag, and N.H. van Dijk: *J. Alloys Compd.*, 2014, vol. 584, pp. 425–29.
15. H. Fang, C.D. Versteylen, S. Zhang, Y. Yang, P. Cloetens, D. Ngan-Tillard, E. Brück, S. van der Zwaag, and N.H. van Dijk: *Acta Mater.*, 2016, vol. 121, pp. 352–64.